Environmental Science & Technology

Article

pubs.acs.org/est

Will Aerosol Hygroscopicity Change with Biodiesel, Renewable Diesel Fuels and Emission Control Technologies?

Diep Vu,[†,‡] Daniel Short,[†,‡] Georgios Karavalakis,[†,‡] Thomas D. Durbin,[†,‡] and Akua Asa-Awuku*[,†,‡,§]

[†]Department of Chemical and Environmental Engineering, Bourns College of Engineering, University of California, Riverside, California 92521, United States

[‡]Bourns College of Engineering, Center for Environmental Research and Technology (CE-CERT), Riverside, California 92507, United States

Supporting Information

ABSTRACT: The use of biodiesel and renewable diesel fuels in compression ignition engines and aftertreatment technologies may affect vehicle exhaust emissions. In this study two 2012 light-duty vehicles equipped with direct injection diesel engines, diesel oxidation catalyst (DOC), diesel particulate filter (DPF), and selective catalytic reduction (SCR) were tested on a chassis dynamometer. One vehicle was tested over the Federal Test Procedure (FTP) cycle on seven biodiesel and renewable diesel fuel blends. Both vehicles were exercised over double Environmental Protection Agency (EPA) Highway fuel economy test (HWFET) cycles on ultralow sulfur diesel (ULSD) and a soy-based biodiesel blend to investigate the aerosol hygroscopicity during the regeneration of the DPF. Overall, the apparent hygroscopicity of emissions during nonregeneration events is consistently low ($\kappa < 0.1$) for all fuels over the FTP cycle. Aerosol emitted during filter regeneration is significantly more CCN active and hygroscopic; average κ values range from 0.242 to 0.439 and are as high as 0.843. Regardless of fuel, the current classification of "fresh" tailpipe emissions as nonhygroscopic remains true during nonregeneration operation. However, aftertreatment technologies such as DPF, will produce significantly more hygroscopic particles during regeneration. To our knowledge, this is the first study to show a significant enhancement of hygroscopic materials emitted during DPF regeneration of on-road diesel vehicles. As such, the contribution of regeneration emissions from a growing fleet of diesel vehicles will be important.

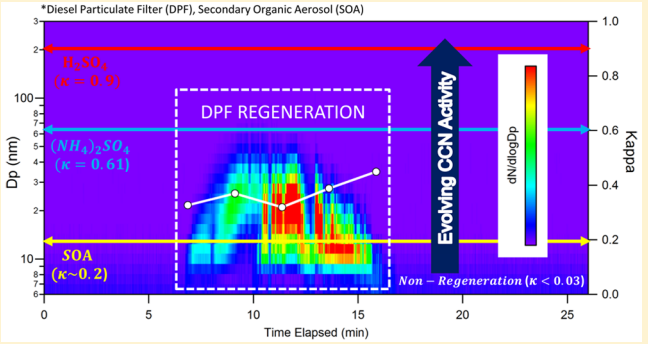

1. INTRODUCTION

Diesel particulate matter (PM) is associated with adverse health effects and is classified as a toxic air contaminant.[1] In an effort to reduce diesel emissions, modern light-duty diesel vehicles are now equipped with robust emission control systems such as diesel oxidation catalysts (DOCs), diesel particulate filters (DPFs), and selective catalytic reduction (SCR) systems that effectively reduce diesel emission rates. However, specific operating conditions may affect particle formation pathways, which consequently modifies particulate composition[2] and potentially enhances the formation of ultrafine semivolatile particles that are not captured by the filtering process.[3] These ultrafine particles make up a small fraction of particulate mass, but represent a large fraction of the overall particle number count. Thus, when considering an equivalent mass concentration, the higher number concentrations of ultrafine particles may be more detrimental to health than larger particles with the same chemically toxic composition.[4,5]

DPFs effectively reduce PM emission rates but require periodic filter regenerations through particulate oxidation to clear or "burn off" the soot that has accumulated on the filter. The temperature of diesel exhaust gases does not always meet the required levels to efficiently oxidize the PM collected in the DPF. As a result, a variety of strategies were developed to help drive the regeneration process, and includes, but is not limited to, using catalyst technology to generate nitrogen dioxide (NO_2) from the oxidation of nitric oxide (NO) to assist in the combustion of soot[6] and using fuel-borne catalysts.[7] During DPF regeneration the vehicle operates under different conditions from those during typical operation and exhaust temperatures can reach above 550 °C.

Several studies have investigated the chemical and physical properties of aerosols formed during the regeneration of DPFs for light-duty diesel passenger vehicles.[8−11] Filter regeneration can produce sharp increases in particle emissions, typically greater by multiple orders of magnitude when compared to nonregeneration operation.[8,10] Slightly elevated particle emissions are also observed immediately after a regeneration event, but regains filtering efficiency when a sufficient amount of soot

Received: August 3, 2016
Revised: December 22, 2016
Accepted: January 3, 2017
Published: January 3, 2017

DOI: 10.1021/acs.est.6b03908
Environ. Sci. Technol. 2017, 51, 1580−1586

builds up on the filter surface again.[12] Evaporation tube measurements by Mohr et al.[12] demonstrated that in spite of the increase in particle concentrations, the nonvolatile solid number concentrations remained fairly consistent between a nonregeneration and a regeneration event. This indicates that the regeneration derived emissions may be dominated by condensed hydrocarbons and less by solid soot. Similarly, Giechaskiel et al.[9] measured the total solid particle number using a particle measurement program (PMP) compliant system and also determined that the emitted exhaust consisted of stored volatile material, but combined with lubricant oil and unburnt fuel. In addition, the regeneration of DPFs can increase the soluble organic fractions.[8] For example, during regeneration, a nucleation mode is typically present; that can be dominated by hydrocarbons and sulfate.[8,13] DOCs can serve as a sulfur trap during normal operating conditions (250 °C), which can then desorb at elevated temperatures[14] during regenerations that can reach above 550 °C.

Although several studies have investigated the changes in the physical and chemical nature of these aerosols derived during the regeneration of DPFs for light-duty diesel passenger vehicles, the potential impact of alternative fuels in addition to diesel emission control systems on aerosol hygroscopicity or its water uptake properties with regards to the cloud condensation nuclei (CCN) budget has not been explored. Fuel-based strategies (e.g., biomass-derived fuels) have been used to mitigate greenhouse gas emissions and address climate change concerns. However, the addition of oxygenated biofuels has been shown to modify the water-soluble organic carbon fractions of diesel emissions.[15,16] There is very limited information in regards to the particle CCN activity and apparent hygroscopicity during DPF regeneration, while it has been shown that the regeneration of DPFs can increase the soluble organic fractions and concentration of water-soluble materials (e.g., sulfates) emitted and that the addition of oxygenated biofuels can modify aerosol hygroscopicity. Thus, their impacts on regional climate and radiative forcing in regards to the CCN budget are not well-known. As a result, the objectives of this study were (a) to examine the impact of fuels on the hygroscopictiy of emissions of modern technology light-duty diesel vehicles, and (b) to evaluate the impact of aftertreatment control devices on the hygroscopicity of particles derived from filter regeneration.

2. EXPERIMENTAL METHODS

2.1. Test Fuels, Vehicles, and Driving Cycles. Seven fuels were used in this study. Fuels include a Federal ultralow sulfur diesel (FED ULSD) and a California Air Recourses Board (CARB) ULSD, and serve as the baseline fuels. Three fatty acid methyl esters (FAMEs), commonly known as biodiesel, produced from soybean oil (SME), animal fat oil (AFME), and waste cooking oil (WCO), respectively, and a hydrogenated vegetable oil (HVO) were utilized as blendstocks to prepare 20 vol % blends with the FED ULSD (FED ULSD/SME-20, FED ULSD/WCO-20, FED ULSD/AFME-20, FED ULSD/HVO-20). Only the WCO biodiesel was used to prepare a 20 vol % blend in the CARB ULSD (CARB ULSD/WCO-20). The main physical and chemical properties of the test fuels are shown in Table S1, Supporting Information.

Two 2012 model year vehicles with direct injection common-rail diesel engines and DOC, DPF, and SCR were used for this study. For confidentiality reasons, the vehicles in this publication will be referred to as Vehicle 1 and Vehicle 2. Vehicle 1 was tested twice over the Federal Test Procedure (FTP) cycle on each of the seven fuels. The FTP consists of three phases: a cold-start phase (Phase 1), transient/stabilized operation (Phase 2), and a hot-start phase (Phase 3). The Vehicles 1 and 2 were tested over two double EPA Highway Fuel Economy Test (HWFET) cycles for FED ULSD and FED/SME-20 to investigate the emissions generated during DPF regeneration. A double HWFET was conducted to provide adequate time for the regeneration to go to completion. Details of the drive cycles and speed traces for the driving cycles are shown in Figure S1 and Figure S2 (Supporting Information). Prior to the first FTP for each of the two regeneration fuels, the DPF was forced to regenerate to eliminate potential artifacts from previous fuels. One baseline double HWFET without a regeneration was conducted for Vehicle 1 on Fed ULSD. A baseline double HWFET for Vehicle 2 is not available. Following the FTPs and the baseline double HWFETs, the vehicles were driven for ∼160 miles, equivalent of 20 LA4 cycles, on road to build up soot in the DPF. The on-road route was designed to simulate the speeds and number of stops in the LA4 portion of the FTP cycle. Double HWFETs were then conducted in a manner where the regenerations were designed to trigger and be completed during the course of the test. For Vehicle 1, the engine control module was programmed to regenerate every 170 miles so that it was ready to regenerate after the soot buildup was completed. Regeneration was triggered manually in the laboratory for Vehicle 2. Details of the regeneration testing protocol are described in Figure S3, Supporting Information. A more detailed description of the fuels, preconditioning protocol, and testing procedures is available in Karavalakis et al.[11]

2.2. Emissions Testing and Instrumentation. All measurements were conducted at the University of California, Riverside (UCR) Center for Environmental Research and Technology (CE-CERT) Vehicle Emissions Research Laboratory (VERL). For certification quality measurements, VERL is equipped with a 48 in. single roller chassis dynamometer (Burke E. Porter), and a positive displacement pump constant volume sampling (PDP-CVS) system. PM emissions were sampled directly off of the PDP-CVS tunnel (Figure S4, Supporting Information). The exhaust is diluted in the CVS, thus driving the dew point down to levels comparable to the room temperature (10−15 °C). It is noted that additional dilution occurs during sampling further drying particles and thus RH is not expected to strongly effect the CCNC supersaturation measurements. The emissions sampled from the CVS are considered to be an appropriate simulation of ambient conditions.

Supersaturated hygroscopic properties were calculated using online measurements. For the FTP and baseline double HWFET cycles, a TSI, Inc., Engine Exhaust Particle Sizer (EEPS) spectrometer 3090 was operated in parallel with a Droplet Measurement Technologies, Inc., single growth column cloud condensation nuclei counter (CCNC) to obtain aerosol hygroscopicity measurements every second. The EEPS utilizes a unipolar corona charger and multiple electrometers to charge and measure the particles based on electrical mobility diameters. The currents are measured at 10 Hz and full size distributions are averaged second by second for 32 channels between 5.6 and 560 nm. Using a continuous-flow thermal gradient diffusion column, the CCNC generates a supersaturated environment for water vapor to condense onto CCN active aerosols to form droplets.[17] The CCNC is operated at a

DOI: 10.1021/acs.est.6b03908
Environ. Sci. Technol. 2017, 51, 1580−1586

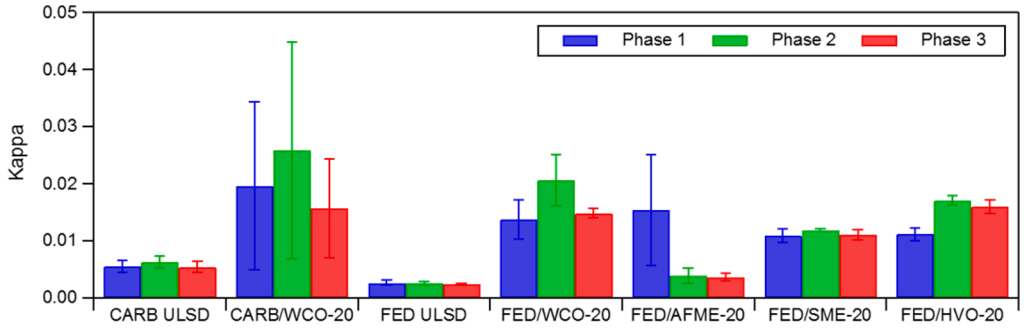

Figure 1. Vehicle 1, measured kappa values for each phase of the FTP for all seven fuels.

total flow rate of 0.5 L/min using a sheath to aerosol flow ratio of 10:1.

For the double HWFET cycles, size resolved aerosol hygrosocopicity was measured using Scanning Mobility CCN Analysis (SMCA).[18] This method characterizes the size resolved aerosol hygroscopic properties every 135 s. Using a TSI 3080 electrostatic classifier, polydisperse aerosols flow through a bipolar krypton-85 charger and are classified based on electrical mobility with a TSI, Inc., 3081L differential mobility analyzer (DMA). Next, the classified or monodisperse aerosol is split between a butanol based condensation particle counter (CPC) (TSI, Inc., 3772) and a CCNC to obtain the total aerosol concentration (CN) and the CCN active aerosol concentration, respectively. The DMA is operated in scanning voltage mode to provide size resolved aerosol hygroscopicity data over a full size distribution. The CCNC is operated at a single critical supersaturation, s_c, for the duration of the cycle. The CCNC was calibrated using aerosolized dry ammonium sulfate, $(NH_4)_2SO_4$, to determine the supersaturations in the column.[18,19]

2.3. Data Analysis. The apparent hygroscopicity is determined every second by deriving the critical activation diameter (D_d) using number size distribution data measured by the EEPS and CCN concentrations measured with the CCNC. A complete description and evaluation of the method is found in Vu et al.;[20] a brief description is provided here. D_d is derived by integrating the aerosol concentration from the largest size bin in the measured size distribution down to a D_d until the particle number concentration agrees with the measured CCN concentrations from the CCNC.

$$N_{CCN(measured)} = -\int_{D_{max}}^{D_d} \frac{dN}{d\log D}(D) d\log D \quad (1)$$

Hygroscopicity calculated from eq 1 has been used in previous studies[20−22] and is applied to the FTP and baseline double HWFET cycles.

In anticipation of the higher concentrations expected from regenerations during the double HWFET, SMCA was utilized to keep the concentration within the counting limitations of the instruments. CCN/CN are measured for a given dry diameter. D_d is determined at the point in which CCN/CN is 0.5.[18]

To describe the water uptake potential of particulate vehicle emissions, a single hygroscopcity parameter, κ, can be used. κ incorporates thermodynamic and physical properties, such as aerosol and water density (ρ_s and ρ_w, respectively), molecular weight of water (M_w), temperature (T), and droplet interfacial surface tension ($\sigma_{s/a}$), to describe particle hygroscopicity. It has been applied in studies to determine the relative hygroscopicity of complex aerosols.[20,22−24] Typical κ ranges include 0 (nonhygroscopic, but wettable), 0.01−0.5 (slightly to very hygroscopic), and >0.5 (significantly hygroscopic, most CCN active).

With s_c, which is derived from the calibration of the CCNC, and D_d derived from one of the two above methods, κ is determined:[25,26]

$$\kappa = \frac{4A^3}{27D_d^3 \ln^2 S_c}, \text{ where } A = \frac{4\sigma_{s/a}M_w}{RT\rho_w} \quad (2)$$

where R is the universal gas constant, and S_c is the critical saturation (>1, defined by $s_c = S_c - 1$). The surface tension of the droplet is assumed to be equivalent to that of pure water. It is noted that the vehicle exhaust emissions may be fractal, which can affect the electrical mobility diameter measurements and subsequent CCN activation.[27,28] However, for the analysis of these emissions, the particles are assumed to be spherical. It is assumed that emissions during nonregeneration are likely organic and fractal and will lower κ measured values. Particles emitted during regeneration are likely dominated by spherical inorganic particles. Mixing state may also modify perceived κ but no mixing state information is available in this study.

3. RESULTS AND DISCUSSION

3.1. Fuel Effects over the FTP: Vehicle 1. The effect of the seven fuels on the hygroscopic properties of fresh vehicle particle emissions operating over the FTP was examined. Size distribution measurements and CCN concentrations were collected for Vehicle 1 using the seven fuels described in Section 2.1. The CCNC was operated at s_c = 0.54% and 0.88% for the transient aerosol tests. Second-by-second aerosol hygroscopicity measurements were used (eq.1).

Overall, the results indicate consistently low apparent hygroscopicities for all fuels (Figure 1). Although subtle, differences were observed between different driving phases; phase 2 produces slightly more hygroscopic particles than phase 1 and phase 3. The least hygroscopic particles are observed for the Fed ULSD (κ = 0.0023 to 0.0026) and the highest for the CARB/WCO-20 blend (κ = 0.0157 to 0.0258). The error bars are the averaged standard deviations obtained from the multiple FTPs for each fuel. The average standard deviation in error associated with the kappa values are relatively small and indicate repeatability between measurements. Detailed kappa results are provided in Table S2 (Supporting Information).

These results are consistent with studies finding fresh vehicle emissions with low hygroscopicity. Size dependent chemical information are unavailable and the lack of mixing state information may contribute some uncertainty to the CCN analysis. However, the results are similar to previously published work that attributed low hygroscopic emissions to

DOI: 10.1021/acs.est.6b03908
Environ. Sci. Technol. 2017, 51, 1580−1586

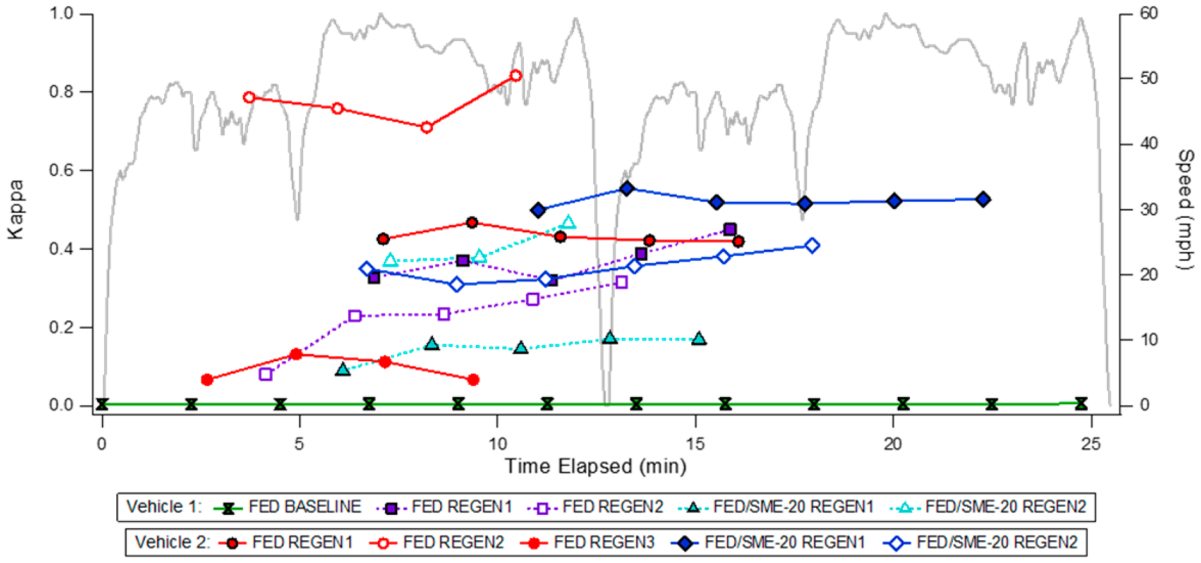

Figure 2. Vehicle 1 and 2 regeneration results using SMCA.- Fed ULSD: one baseline cycle, two cycles with regeneration, and Fed ULSD/SME-20: two cycles with regeneration. Vehicle 2, Fed ULSD: three cycles with regeneration, and Fed ULSD/SME-20: two cycles with regeneration. The double HWFET speed trace is provided in gray. Measured hygroscopicity during nonregeneration events are ~0 (not shown).

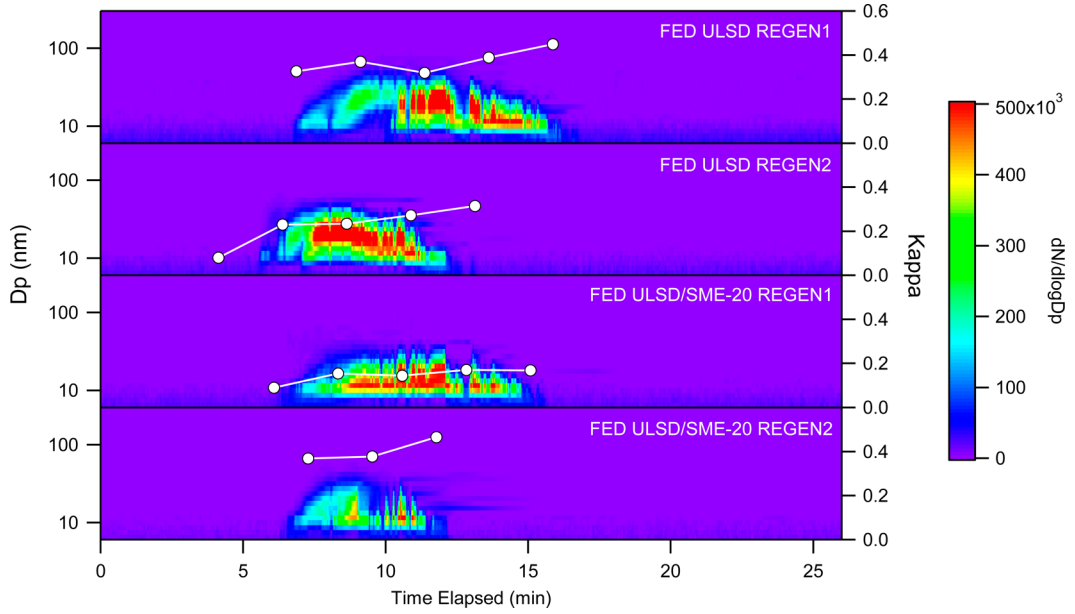

Figure 3. Vehicle 1 Regenerations. Particle size distributions shown (left axis) and kappa (right axis) as a function of time elapsed.

an externally mixed state where soluble materials are less likely to condense, insoluble material present in the aerosols (e.g., soot), and small sizes where a majority of the aerosols exist in the nucleation mode.[20,29−34] When comparing the overall apparent hygroscopicity of particles over the FTP, the results show relatively low hygroscopicity in relation to more hygroscopic species from secondary organics ($\kappa \sim 0.2$) and inorganic aerosol species like ammonium sulfate ($\kappa = 0.61$).

3.2. Baseline Effects over the Double HWFET: Vehicle 1. A baseline double HWFET was performed for Vehicle 1 on Fed ULSD with no regeneration. Hygroscopicity is calculated every second (eq 2) during baseline testing. Overall, the apparent particle hygroscopicity was low throughout the baseline test (κ = 0.0023 to 0.0026) (Figure 2). This range of kappa values is similar to kappa values measured during the FTP cycles for this vehicle.

3.3. Regeneration Effects over the Double HWFET: Vehicle 1 and 2. Regeneration testing was performed on Vehicle 1 and Vehicle 2 on Fed ULSD and Fed/SME-20 over the double HWFET cycles. Two double HWFET regeneration tests were performed for each of the two fuels with the exception of Vehicle 2, which had three tests on the Fed ULSD. The CCNC was operated at s_c = 0.69% and 0.91% for the transient aerosol tests. SMCA was used to characterize the hygroscopicity properties. These results are summarized in Figure 2 with detailed kappa results in Tables S3 and S4 (Supporting Information).

For Vehicle 1 and 2 the regenerations lasted approximately 7−12 min and 11−22 min, respectively. The length of regeneration and the amount of PM emitted can vary as they are a function of the driving patterns of the vehicle (e.g., steady-state high speed cycles) and mileage accumulation.[10] All

DOI: 10.1021/acs.est.6b03908
Environ. Sci. Technol. 2017, 51, 1580−1586

regeneration events were signified by elevated exhaust emissions and exhaust temperatures for both vehicles. Size and concentration data (EEPS) are only available for Vehicle 1 (Figure 3). A large nucleation mode is observed, which is consistent with other studies conducting regenerations.[13] The fuels are not observed to affect the size distributions.

The highest hygroscopicity is observed for the aerosols emitted during regeneration for both vehicles and both fuels; with average κ values ranging from 0.242 to 0.434 (Figure 4).

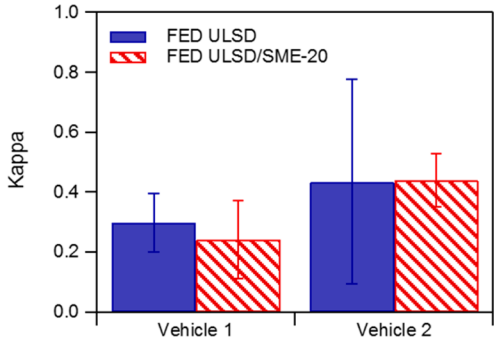

Figure 4. Average Kappa values for the regeneration events.

The highest and lowest hygroscopicity was observed for Vehicle 2 on the FED ULSD (κ = 0.843 and κ = 0.0661). Additional kappa values are available in Table S3, S4, and S5 (Supporting Information). The higher kappa values may be attributed to the higher amount of sulfates released during regeneration (derived from sulfur on the soot particles, sulfur in the DPF). This is consistent with the findings from Bikas and Zervas[8] who observed an increase in the nucleation nanoparticles, which consisted mostly of HC or sulfates during the regeneration of a noncatalyzed SiC filter and a Pt catalyst retrofitted on a passenger car equipped with a 1.9 L diesel Euro4 engine. They also found that soluble organic fractions increased during regeneration from 0 to 50%, which were determined to be composed of hydrocarbons with 77% from fuel and the remaining 23% from engine oil. In addition, sulfates made up 12% of the total PM (from 3% before regeneration) and were correlated with increased fuel consumption, higher DPF temperatures, increased sulfate concentrations with larger diameter particles (median diameter of 40 nm). Both vehicles 1 and 2 had lower fuel economy during the DPF regenerations,[11] thereby increasing the amount of sulfur due to increased fuel consumption.

Sulfur may play an important role in elevating aerosol emission hygroscopicity. To drive the regeneration, ULSD may be injected to lower the required DPF temperatures for regeneration. An increase in fuel consumption during regeneration measurements can result in an increase in SO_2.[8] Studies suggest that SO_2 may be oxidized to SO_3 in the catalyst and lead to the formation of sulfate particles in the nucleation mode.[2] DOCs can serve as a sulfur trap and store a large fraction of the emitted SO_2; which can oxidize to form SO_3. This can then form sulfuric acid in the presence of water or sulfates with metal oxides (e.g., alumina, titania, zirconia) on the surface of the DOC.[14] This process is irreversible and the sulfuric acid/SO_x can begin desorbing at temperatures as low as 250 °C.[14] Sulfuric acid is very hygroscopic, with a reported kappa value of 0.9.[26] If mixed with less soluble materials, sulfuric acid may greatly modify the CCN activity. Aerosols internally mixed with sulfuric acid vapor can be highly hygroscopic.[35] The observed large kappa values (>0.8) may be due to sulfuric acid or interactions of SO_x with water vapor in the exhaust or the CCN. It should also be noted that SCR systems use urea to reduce NO_x, ammonia slip may be occurring due to the urea injection system. This ammonia may potentially react with sulfuric acid to form ammonium sulfate, which has a kappa value of 0.61.[26]

This is the first study to investigate the supersaturated hygroscopic properties of particle emissions derived from the regeneration of DPFs while operating on commercially available ULSDs and biodiesel blends. For the FTP tests for Vehicle 1, although subtle, the changes in kappa indicate the sensitivity of the chemical composition to the different renewable and biodiesel fuels and the transient nature of the drive cycle. Overall, kappa values of these emissions are less than 0.03 and did not display any order of magnitude differences in value; emissions directly from the tail-pipe exhibit low kappa values and are consistent with fresh vehicle aerosol emissions typically classified as nonhygroscopic.

Regeneration will produce significantly more particle emissions and modify the aerosol composition from non-hygroscopic to hygroscopic. DPF Regeneration has a stronger impact on particle emissions than modifying fuels. The particle hygroscopicity during regeneration was considerably higher than that of the nonregeneration cycles; reaching average kappa values of 0.242 to 0.434, but upward of 0.843. This indicates the presence of highly soluble materials, which may greatly affect the water uptake properties of compounds that are insoluble.[36]

DPF regeneration increases both particle number and hygroscopicity. The potential impact of modifying a significant fraction of the modern vehicle fleet with diesel engine technologies such as DPFs may have unforeseen environmental consequences. Vehicle emissions are traditionally characterized as nonhygroscopic in radiative forcing estimates and the results of the biodiesel and renewable diesel fuel blends utilized in this study further supports this phenomenon, as no significant fuel effects were observed and the majority of the PM emissions were collected by the filter. However, during the oxidation and regeneration process, the particle number and hygroscopic properties were greatly modified and a significant increase in water uptake was observed. Although it is difficult to quantify the overall CCN contribution due to the varying levels of hygrosocopicity, intensity and duration of regeneration events, current emissions testing that does not incorporate regeneration is not fully representative of the emissions from modern diesel vehicles equipped with robust emission control technologies. As more vehicles continue to utilize this technology, the impact on local health, regional visibility, and climate due to the application of robust emission control systems becomes increasingly important and should be evaluated in future studies.

■ ASSOCIATED CONTENT

Supporting Information

The Supporting Information is available free of charge on the ACS Publications website at DOI: 10.1021/acs.est.6b03908.

Data used in this study and additional figures are available in Supporting Information. There are three figures, which include two speed traces for the test cycles (FTP and double HWFET), and regeneration emissions testing protocol diagram. The tables include the physical

DOI: 10.1021/acs.est.6b03908
Environ. Sci. Technol. 2017, 51, 1580−1586

and chemical properties of the test fuels and the numerical values for the Figures 1, 2, and 4 (PDF)

AUTHOR INFORMATION

Corresponding Author

*Phone: (301) 405-8527; e-mail: asaawuku@umd.edu.

ORCID

Akua Asa-Awuku: 0000-0002-0354-8368

Present Address

§(A.A.-A.) A. James Clark School of Engineering, Chemical and Biomolecular Engineering, University of Maryland, College Park, Maryland 20742, United States.

Notes

The authors declare no competing financial interest.

ACKNOWLEDGMENTS

Vehicle testing in this study was substantially supported by the Coordinating Research Council (CRC) (Project No. AVFL-17b). Aerosol hygroscopicity work was supported by the National Science Foundation Award (1151893). D.V. acknowledges support from the U.S. Environmental Protection Agency STAR Fellowship (FP-91751101). This work is the sole responsibility of the grantee and does not represent the official views of any funding agencies. D.S. acknowledges support from the University of California Transportation Center Graduate Fellowship. The authors additionally thank Kurt Bumiller and Mark Villela for their technical contribution during vehicle testing.

REFERENCES

(1) CARB, 1999, Toxic Air Contaminant Identification List, Title 17, CCR, § 93000. Substances Identified As Toxic Air Contaminants; http://www.arb.ca.gov/toxics/id/taclist.htm.

(2) Biswas, S.; Verma, V.; Schauer, J.; Sioutas, C. Chemical speciation of PM emissions from heavy-duty diesel vehicles equipped with diesel particulate filter (DPF) and selective catalytic reduction (SCR) retrofits. *Atmos. Environ.* **2009**, *43*, 1917−1925.

(3) Sioutas, C. *Final Report: Physiochemical and Toxicological Assessment of the Semi-Volatile and Non-Volatile Fraction of PM from Heavy-Duty Vehicles Operating with and without Emissions Control Technologies*, 2011

(4) Zhu, Y.; Hinds, W.; Kim, S.; Sioutas, C. Concentration and Size Distribution of Ultrafine Particles Near a Major Highway. *J. Air Waste Manage. Assoc.* **2002**, *52*, 1032−1042.

(5) Valavanidis, A.; Fiotakis, K.; Vlachogianni, T. Airborne particulate matter and human health: Toxicological assessment and importance of size and composition of particles for oxidative damage and carcinogenic mechanisms. *Journal of Environmental Science and Health - Part C. Environmental Carcinogenesis and Ecotoxicology Reviews* **2008**, *26*, 339−362.

(6) Cooper, B.; Jung, H.; Thoss, J. *Treatment of Diesel Exhaust Gases*, United States Patent; 4902487. Johnson Matthey, Inc., Valley Forge, Pa. February 20, 1990.

(7) Blanchard, G.; Colignon, C.; Griard, C.; Rigaudeau, C.; Slavat, O.; Seguelong, T. Passenger Car Series Application of a New Diesel Particulate Filter System Using a New Ceria-Based Fuel-Borne Catalyst: From the Engine Test Bench to European Vehicle Certification. *SAE Tech. Pap. Ser.* 2002−01−2781; **2002**; doi:10.4271/2002-01-2781.

(8) Bikas, G.; Zervas, E. Regulated and Non-Regulated Pollutants Emitted during the Regeneration of Diesel Particulate Filter. *Energy Fuels* **2007**, *21*, 1543−1547.

(9) Giechaskiel, B.; Munoz-Bueno, R.; Rubino, L.; Manfredi, U.; Dilara, P.; De Santi, G.; Andersson, J. Particle Measurement Programme (PMP): Particle Size and Number Emissions Before, During and After Regeneration Events of a Euro 4 DPF Equipped Light-Duty Diesel Vehicle. *SAE Tech. Pap. Ser.* 2007−01 1944; doi:2007**10.4271/2007-01-1944**.

(10) Dwyer, H.; Ayala, A.; Zhang, S.; Collins, J.; Huai, T.; Herner, J.; Chau, W. Emissions from a diesel car during regeneration of an active diesel particulate filter. *J. Aerosol Sci.* **2010**, *41*, 541−552.

(11) Karavalakis, G.; Durbin, T.; Russell, R. CRC Final Project Report: CRC Project No. AVFL − 17b: Biodiesel and Renewable Diesel Characterization and Testing in Modern LD Diesel Passenger Cars and Trucks. 2014.

(12) Mohr, M.; Forss, A.; Lehmann, U. Particle Emissions from Diesel Passenger Cars Equipped with a Particle Trap in Comparison to Other Technologies. *Environ. Sci. Technol.* **2006**, *40*, 2375−2383.

(13) Maricq, M. Chemical characterization of particulate emissions from diesel engines: A review. *J. Aerosol Sci.* **2007**, *28*, 1079−1118.

(14) Kröcher, O.; Widmer, M.; Elsener, M.; Rothe, D. Adsorption and Desorption of SO_x on Diesel Oxidation Catalysts. *Ind. Eng. Chem. Res.* **2009**, *48*, 9847−9857.

(15) Cheung, K. L.; Polidori, A.; Ntziachristos, L.; Tzamkiozis, T.; Samaras, Z.; Cassee, F. R.; Gerlofs, M.; Sioutas, C. Chemical Characteristics and Oxidative Potential of Particulate Matter Emissions from Gasoline, Diesel, and Biodiesel Cars. *Environ. Sci. Technol.* **2009**, *43*, 6334−6340.

(16) Happonen, M.; Heikkilä, J.; Aakko-Saksa, P.; Murtonen, T.; Lehto, K.; Rostedt, A.; Sarjovaara, T.; Larmi, M.; Keskinen, J.; Virtanen, A. Diesel exhaust emissions and particle hygroscopicity with HVO fuel-oxygenate blend. *Fuel* **2013**, *103*, 380−386.

(17) Roberts, G. C.; Nenes, A. A Continuous-Flow Streamwise Thermal-Gradient CCN Chamber for Atmospheric Measurements. *Aerosol Sci. Technol.* **2005**, *39*, 206−221.

(18) Moore, R. H.; Nenes, A.; Medina, J. Scanning Mobility CCN Analysis - A Method for Fast Measurements of Size-Resolved CCN Distributions and Activation Kinetics. *Aerosol Sci. Technol.* **2010**, *44*, 861−871.

(19) Rose, D.; Gunthe, S. S.; Mikhailov, E.; Frank, G. P.; Dusek, U.; Andreae, M. O.; Pöschl, U. Calibration and measurement uncertainties of a continuous-flow cloud condensation nuclei counter (DMT-CCNC): CCN activation of ammonium sulfate and sodium chloride aerosol particles in theory and experiment. *Atmos. Chem. Phys.* **2008**, *8*, 1153−1179.

(20) Vu, D.; Short, D.; Karavalakis, G.; Durbin, T. D.; Asa-Awuku, A. Integrating cloud condensation nuclei predictions with fast time resolved aerosol instrumentation to determine the hygroscopic properties of emissions over transient drive cycles. *Aerosol Sci. Technol.* **2015**, *49*, 1149−1159.

(21) Kammermann, L.; Gysel, M.; Weingartner, E.; Herich, H.; Cziczo, D. J.; Holst, T.; Svenningsson, B.; Arneth, A.; Baltensperger, U. Subarctic atmospheric aerosol composition: 3. Measured and modeled properties of cloud condensation nuclei. *J. Geophys. Res.* **2010**, *115*, D04202.

(22) Jurányi, Z.; Gysel, M.; Weingartner, E.; Bukowiecki, N.; Kammermann, L.; Baltensperger, U. A 17 month climatology of the cloud condensation nuclei number concentration at the high alpine site Jungfraujoch. *J. Geophys. Res.* **2011**, *116*, D10.

(23) Asa-Awuku, A.; Moore, R. H.; Nenes, A.; Bahreini, R.; Holloway, J. S.; Brock, C. A.; Middlebrook, A. M.; Ryerson, T. B.; Jimenez, J. L.; DeCarlo, P. F.; Hacobian, A.; Weber, R. J.; Stickel, R.; Tanner, D. J.; Huey, L. G. Airborne cloud condensation nuclei measurements during the 2006 Texas Air Quality Study. *J. Geophys. Res.* **2011**, *116*, D11201.

(24) Engelhart, G. J.; Asa-Awuku, A.; Nenes, A.; Pandis, S. N. CCN activity and droplet growth kinetics of fresh and aged monoterpene secondary organic aerosol. *Atmos. Chem. Phys.* **2008**, *8*, 3937−3949.

(25) Köhler, H. The nucleus in and the growth of hygroscopic droplets. *Trans. Faraday Soc.* **1936**, *32*, 1152−1161.

(26) Petters, M. D.; Kreidenweis, S. M. A single parameter representation of hygroscopic growth and cloud condensation nucleus activity. *Atmos. Chem. Phys.* **2007**, *7*, 1961−1971.

DOI: 10.1021/acs.est.6b03908
Environ. Sci. Technol. 2017, 51, 1580−1586

(27) Nakao, S.; Shrivastava, M.; Nguyen, A.; Jung, H.; Cocker, D., III Interpretation of Secondary Organic Aerosol Formation from Diesel Exhaust Photo-oxidation in an Environmental Chamber. *Aerosol Sci. Technol.* **2011**, *45*, 954−962.
(28) Giordano, M.; Espinoza, C.; Asa-Awuku, A. Experimentally measured morphology of biomass burning aerosol and its impacts on CCN ability. *Atmos. Chem. Phys.* **2015**, *15*, 1807−1821.
(29) Dua, S.; Hopke, P.; Raunemaa, T. Hygroscopicity of diesel aerosols. *Water, Air, Soil Pollut.* **2009**, *112*, 247−257.
(30) Weingartner, E.; Burtscher, H.; Baltensperger, U. Hygroscopic properties of carbon and diesel soot particles. *Atmos. Environ.* **1997**, *31*, 2311−2327.
(31) Hasegawa, S.; Ohta, S. Some measurements of the mixing state of soot-containing particles at urban and non-urban sites. *Atmos. Environ.* **2002**, *36*, 3899−3908.
(32) Andreae, M. O.; Rosenfeld, D. Aerosol−cloud−precipitation interactions. Part 1. The nature and sources of cloud-active aerosols. *Earth-Sci. Rev.* **2008**, *89*, 13−41.
(33) Rose, D.; Gunthe, S. S.; Su, H.; Garland, R. M.; Yang, H.; Berghof, M.; Cheng, Y. F.; Wehner, B.; Achtert, P.; Nowak, A.; Wiedensohler, A.; Takegawa, N.; Kondo, Y.; Hu, M.; Zhang, Y.; Andreae, M. O.; Pöschl, U. Cloud condensation nuclei in polluted air and biomass burning smoke near the mega-city Guangzhou, China − Part 2: Size-resolved aerosol chemical composition, diurnal cycles, and externally mixed weakly CCN-active soot particles. *Atmos. Chem. Phys.* **2011**, *11*, 2817−2836.
(34) Tritscher, T.; Juranyi, Z.; Martin, M.; Chirico, R.; Gysel, M.; Heringa, M. F.; DeCarlo, P. F.; Sierau, B.; Prevot, A. S. H.; Weingartner, E.; Baltenspreger, U. Changes of hygroscopicity and morphology during ageing of diesel soot. *Environ. Res. Lett.* **2011**, *6*; doi:03402610.1088/1748-9326/6/3/034026.
(35) Khalizov, A. F.; Zhang, R.; Zhang, D.; Xue, H.; Pagels, J.; McMurry, P. H. Formation of highly hygroscopic soot aerosols upon internal mixing with sulfuric acid vapor. *J. Geophys. Res.* **2009**, *114*, D05208.
(36) Bilde, M.; Svenningsson, B. CCN activation of slightly soluble organics: The importance of small amounts of inorganic salt and particle phase. *Tellus, Ser. B* **2004**, *56B*, 128−134.

DOI: 10.1021/acs.est.6b03908
Environ. Sci. Technol. 2017, 51, 1580−1586